

The Soret effect in laser-irradiated quartz (liquid phase)

This article has been downloaded from IOPscience. Please scroll down to see the full text article.

1989 J. Phys.: Condens. Matter 1 3363

(<http://iopscience.iop.org/0953-8984/1/21/007>)

View [the table of contents for this issue](#), or go to the [journal homepage](#) for more

Download details:

IP Address: 94.79.44.176

The article was downloaded on 10/05/2010 at 18:11

Please note that [terms and conditions apply](#).

LETTER TO THE EDITOR

The Soret effect in laser-irradiated quartz

Antonio Miotello

Dipartimento di Fisica and Centro Interuniversitario Struttura della Materia, I-38050 Povo, Trento, Italy

Received 20 March 1989

Abstract. The laser-induced evolution of concentration profiles of Si implanted into quartz is described in terms of ordinary and Soret migration in a SiO₂ liquid phase. Heat- and particle-transport equations are numerically integrated. The result obtained for the Soret coefficient is discussed in the framework of the Bhat and Swalin theory.

Nano-, pico- and femtosecond laser pulses irradiating metals and semiconductors (Si in particular) provide a unique tool for investigating many non-equilibrium phenomena occurring in both the solid and liquid phase in ultra-short interval times. As to the laser-induced solid-state rate processes, primary importance is attached to femtosecond laser pulses inducing electron-gas excitation in metals [1]. Indeed, since electron-phonon collision times are of the order of 10^{-14} s at room temperature, several collisions between hot electrons (>1 eV) and phonons (≈ 0.2 eV) are required for electron-lattice equilibration. Hence excited electrons survive for long time (on the scale of the Debye frequency) and so the dynamics of excited hot electrons may be studied through, for example, the changes in the optical properties of the irradiated metals [1].

Concerning the liquid-phase rate processes we here recall the laser-induced liquid-amorphous phase transitions and the laser-induced crystal-growth velocities in the m s^{-1} regime for which many new aspects for segregation and trapping of impurity atoms have been pointed out [2–4].

In connection with these laser-induced liquid-phase rate processes, an interesting transport effect is Soret migration, seen only in metals to date. In particular, thermal migration is seen to occur in the opposite direction with respect to the temperature gradients [5, 6].

The aim of this Letter is to prove for the first time that the laser-induced Soret effect occurs also in non-metals and in a direction parallel to the temperature gradients. The starting point of our analysis is the experimental results of Shimizu *et al* [7].

Suprasil fused quartz was implanted with 50 and 180 keV Si⁺ to a nominal dose of 5×10^{17} ions cm^{-2} . Implanted specimens were then irradiated with 20 ns laser pulses (wavelengths 308 and 575 nm) with energy density in the range 200–1170 mJ cm^{-2} . The authors [7] discussed the Si profiles evolution in terms of Si thermal migration, in the solid phase, arising from a temperature gradient induced by non-uniform optical absorption. However, no quantitative analysis of either thermal-energy transport in laser-irradiated SiO₂ or of Si atomic transport has been performed [7].

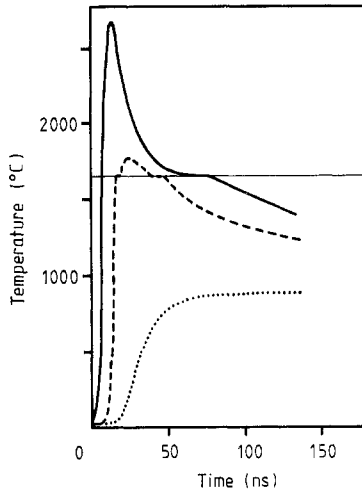


Figure 1. Temperature evolution in SiO₂, as a function of time for three selected depths; full curve: 150 nm; dashed curve: 300 nm; dotted curve: 500 nm. The energy of the laser pulse is 200 mJ cm⁻² (50 keV ions implant) and ϕ (see equation (2)) is 2.1×10^{-17} cm².

First let us prove that the changes occurring for Si profiles after laser irradiations are connected to an Si transport process in a liquid phase of the SiO₂ and not in a solid phase as suggested by Shimizu *et al* [7]. Indeed, the heat transport equation (in a one-dimensional form which is appropriate to our case [8, 9]) is:

$$c\rho \partial T/\partial x = (\partial/\partial x)(K(T) \partial T/\partial x) + A(x, t) \quad (1)$$

where x is the coordinate of the axis normal to the sample surface ($x = 0$ is the surface position), t is the time, ρ is the SiO₂ density, c the specific heat, K the thermal conductivity and $A(x, t)$ the heat-source term. In the actual case

$$A(x, t) = \phi n(x)F(t) \exp\left(-\phi \int_0^x n(x') dx'\right) \quad (2)$$

where $F(t)$ is the incident power density, $n(x)$ is the concentration (atoms cm⁻³) of implanted Si ions and ϕ is the optical absorption cross section of a Si atom implanted into SiO₂. Boundary conditions for (1) are discussed in [8]. Here we only report the boundary condition which holds at the liquid–solid interface:

$$K_{\text{sol}} \partial T/\partial x|_{x^+} - K_{\text{liq}} \partial T/\partial x|_{x^-} = H\rho dx/dt \quad (3)$$

where H is the latent heat of fusion.

By using the available thermodynamic data [10] in equations (1)–(3), together with the experimental data for ϕ and $n(x)$, we solved the heat equation according to the numerical procedure described in [8]. In figure 1 we report the temperature–time evolution at three different depths of the irradiated SiO₂. The energy of the laser pulse is 200 mJ cm⁻² (the lower one employed in [7]). Notice that melting occurs up to a depth of about 300 nm. The dynamical behaviour of the melting–resolidification process is best

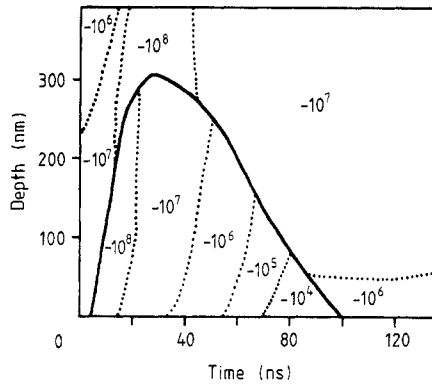


Figure 2. Time evolution of the solid–liquid interface (full curve) in laser-irradiated SiO₂ (see caption of figure 1 for details). Average values of the temperature gradients are indicated.

illustrated in figure 2, where we report $x(t)$ of equation (3) and indicative values for the temperature gradients. These last quantities, along with the interval-time duration of the melting–resolidification process, are the relevant parameters for a theoretical description of the Si atomic transport. Notice that the time duration of the laser pulse (20 ns) is quite small ($\frac{1}{3}$) with respect to the overall duration of the molten phase, where the observed changes of Si profiles occur, and so we do not include time evolution of $n(x)$ in the absorption term (2).

Before illustrating the theoretical results for the Si atomic transport we observe that for the extreme values of the laser pulse energies (580 mJ cm⁻² for 50 keV implant and 1170 mJ cm⁻² for 180 keV implant) a quite-relevant vaporisation process of the SiO₂ matrix is expected. However, in this Letter we do not investigate this phenomenon. Indeed, its quantitative description requires a knowledge of processes involved in laser–gas interaction including gas breakdown phenomena: up to now these processes are not well characterised for laser–SiO₂ interaction. The continuity equation for Si impurity concentration, including both ordinary and Soret migration, is [5]

$$\partial n / \partial t = D(\partial^2 n / \partial x^2) + DS_T(\partial n / \partial x)(\partial T / \partial x) + DS_T n(\partial^2 T / \partial x^2) \quad (4)$$

where $n = n(x, t)$ is the Si impurity concentration at depth x and time t and $S_T = D' / D$ (D is the ordinary diffusion coefficient and D' is the thermal migration coefficient). Generally the last term in equation (4) plays only a minor role in the dynamics of the Soret migration [5, 6] but, as we shall see below, in the actual case of laser-induced melting in non-metals a relevant contribution stems also from the term $\partial^2 T / \partial x^2$. In the numerical integration of equation (4) we take time-independent temperature gradients by considering appropriate average values in the liquid phase.

Notice that (this is evident in figure 2) in general, temperature gradients near the surface of the irradiated SiO₂ (within 50–100 nm in the surface layers) are lower than that pertinent to larger depths. We account for this fact by simply taking an appropriate average value of $\partial T / \partial x$ near the surface layers (≤ 60 nm) less than that of larger depths.

In figure 3 we report, along with the experimental results, the theoretical profiles calculated by integration of equation (4) and fitting procedures. Notice that just through the discontinuity of the temperature gradients we are able to reproduce all features of

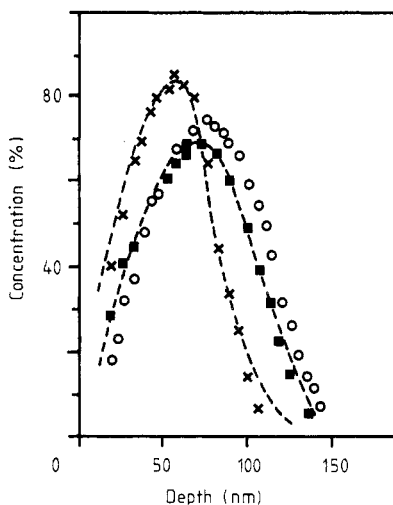


Figure 3. Open circles: as-implanted Si profile (50 keV ions implantation). Squares: Si profile after a laser pulse of 200 mJ cm^{-2} . Crosses: Si profile after a laser pulse of 360 mJ cm^{-2} . Dashed curves: theoretical profiles calculated by integration of equation (4) (see text).

the experimental profile obtained with a laser-pulse energy of 360 mJ cm^{-2} (50 keV Si^+ implant) where the peak of the impurity profile is observed to increase: this is a peculiarity connected to a discontinuity in atomic fluxes.

For the other experimental peaks this fact is not so evident since either the duration of the molten phase is lower (50 keV implant, 200 mJ cm^{-2}) or the much more in-depth-implanted Si^+ impurities allow for a more uniform distribution of the thermal energy (180 keV Si^+ implants).

All the experimental results (for simplicity we do not report calculated profiles pertinent to 180 keV implants) are reproduced with $S_T = -0.2 \text{ K}^{-1}$ and D of the order of $10^{-5} \text{ cm}^2 \text{ s}^{-1}$. This means that all the observed differences in experimental profiles are connected to the different thermodynamic behaviour of the laser-irradiated quartz.

While the obtained D -value is consistent with liquid-diffusivity data, the S_T -value is quite large, but comparable with that quoted for the laser-induced Soret effect in metals, the sign being opposite [5, 6]. The heat of transport turns out to be $\approx -10^6 \text{ cal mol}^{-1}$.

In discussing the results obtained for S_T we would like to stress that none of the existing models for the Soret effect is generally accepted, the cross-coefficients in transport processes being actually open problems in the field of condensed matter. However, an interesting point emerges when we are looking at the Bhat and Swalin [11] theory for liquid metals. Indeed, in this theory the heat of transport is composed of two parts, one of which arises from the interaction of the conduction electrons with solute ions and the other (which is relevant for our situation) from the interaction of the diffusing ions with solute ones. The latter can be calculated by assuming that the liquid is a dense gas and applying the thermo-transport theory in binary gas mixtures. The sign of this part is determined primarily by the mass differences, the lighter impurity migrating to the warmer end. With this in mind, notice that the Si impurities migrate towards the warmer region and this is consistent with the Bath and Swalin [11] theory. In conclusion, while the value of the DS_T parameter is consistent with that evaluated for the laser-induced Soret effect in metals, we think that an explanation of this value from first principles is a paramount problem whose solution is probably also connected to the possibility of performing a systematic analysis of a possible laser-induced Soret effect in many impurity-matrix combinations.

References

- [1] Brorson S D, Fujimoto J G and Ippen E P 1987 *Phys. Rev. Lett.* **59** 1962
- [2] Cullis A G, Webber H C, Chew N G, Poate J M and Baeri P 1982 *Phys. Rev. Lett.* **49** 219
- [3] Spaepen F and Turnbull D 1979 *Laser-Solid Interactions and Laser Processing* ed. S D Ferris, H J Leamy and J M Poate (New York: AIP) p 73
- [4] White C W, Wilson S R, Appleton B R and Young F W 1980 *J. Appl. Phys.* **51** 738
- [5] Miotello A, Dona'dalle Rose L F and Desalvo A 1982 *Appl. Phys. Lett.* **40** 135
- [6] Miotello A and Dona'dalle Rose L F 1982 *Phys. Lett.* **87A** 317
- [7] Shimizu T, Itoh N and Matsunami N 1988 *J. Appl. Phys.* **64** 3663
- [8] Dona'dalle Rose L F and Miotello A 1980 *Radiat. Eff.* **53** 7
- [9] Dona'dalle Rose L F and Miotello A 1980 *Radiat. Eff.* **53** 19
- [10] *The Oxide Handbook* 1973 ed. G S Samsonov (New York: Plenum)
- [11] Bhat B N and Swalin R A 1972 *Acta Metall.* **20** 1387